Na^+ / Ca^{2+} selectivity in the bacterial voltage-gated sodium channel NavAb

The recent publication of a number of high resolution bacterial voltage-gated sodium channel structures has opened the door for the mechanisms employed by these channels to distinguish between ions to be elucidated. The way these channels select between Na^+ and K^+ has been investigated in computational studies, but the selectivity for Na^+ over Ca^{2+} has not yet been studied in this way. Here we use molecular dynamics simulations to calculate the energetics of Na^+ and Ca^{2+} transport through the channel. Single ion profiles show that Ca^{2+} experiences a large barrier midway through the selectivity filter that is not seen by Na^+. This barrier is caused by the need for Ca^{2+} to partly dehydrate to pass through this region and the lack of compensating interactions with the protein. Multi-ion profiles show that ions can pass each other in the channel, which is why the presence of Ca^{2+} does not block Na^+ conduction despite binding more strongly in the pore.

Ben Corry

Research School of Biology
The Australian National University
Acton, ACT, 0200
Australia

ben.corry@anu.edu.au
+61 2 61250842

Introduction:

Voltage-gated sodium channels create the upstroke of action potentials in excitable cells by opening a Na^+ selective transmembrane pore in response to small depolarising signals. (Catterall, 2000; Goldin, 2001; Hille, 2001) These channels are able to rapidly move Na^+ ions down their electrochemical gradient, while limiting the passage of other ions such as K^+, Ca^{2+} and Cl^-. Until recently, gaining a detailed understanding of the mechanisms leading to ion selectivity in these channels has been difficult due to a lack of structural information. The publication of atomic resolution structures of a number of voltage-gated sodium channels from bacteria in the last 18 months (McCusker, et al., 2012; Payandeh, et al., 2012; Payandeh, et al., 2011; Zhang, et al., 2012) has, however, now made it possible to elucidate the physical mechanisms employed to generate sodium selectivity.

Unlike eukaryotic sodium channels that are formed from a single protein chain, the bacterial sodium channels are made up of four identical subunits that surround a central pore. The pore shape is similar to the familiar structure of potassium channels. One set of transmembrane helices form an inverted tepee that lines the inner half of the pore and contains the activation gate. A re-entrant loop between two short helices forms a narrow 'selectivity filter' that is wider and shorter than that of potassium channels, as well as being partly lined by amino acid side chains. In these bacterial sodium channels, four identical subunits line the pore and the external end of the filter is surrounded by side chains of four glutamate residues (Glu177), in the same sequence position as the characteristic DEKA ring found in eukaryotic sodium channels (Payandeh, et al., 2011) which is known from mutation studies to be essential in creating Na^+ selectivity. (Favre, et al., 1996; Heinemann, et al., 1992; Sun, et al., 1997)

The question of how the bacterial sodium channels can discriminate between Na^+ and K^+ has been addressed in studies based upon the crystal structure of the channel from *Arcobacter butzleri* (NavAb).(Payandeh, et al., 2011) It was initially suggested that the high field strength of the glutamate residues would create an ion binding site more favourable for Na^+ than K^+.(Payandeh, et al., 2011) Two computational studies, however, highlighted the importance of a narrow region just beyond this binding site for creating selectivity.(Corry and Thomas, 2012; Furini and Domene, 2012) We have suggested that the discrimination at this point arises from the inability of K^+ to fit through the narrow region of the pore along with surrounding water molecules in the optimal geometry. (Corry and Thomas, 2012)

How ion channel discriminate between Na^+ and Ca^{2+} is also not straight forward to explain. The family of voltage-gated sodium channels is closely related to the voltage-gated calcium channels. They share a similar topology comprising four homologous domains each containing 6 transmembrane sections. Furthermore, both classes of channel are believed to share some structural features in the selectivity filter.(Hille, 2001) Mutation of a few key residues in both eukaryotic and bacterial sodium channels can decrease or reverse Na^+ selectivity to create a pore with characteristics similar to the voltage-gated calcium channels (Heinemann, et al., 1992; Shaya, et al., 2011; Sun, et al., 1997; Yue, et al., 2002). Similarly, substitutions in the conserved 'EEEE locus' of calcium selective channels can allow Na^+ permeation or remove Ca^{2+} currents (Cibulsky and Sather, 2000; Ellinor, et al., 1995; Tang, et al., 1993). Thus the difference in selectivity seen in sodium and calcium channels appears to be due to only minor differences in the protein.

A number of computational studies made in the absence of atomic resolution information have examined the nature of selection between Na^+ and Ca^{2+}.(Boda, et al., 2009; Corry, et al., 2000; Corry, et al., 2001; Corry and Chung, 2006; Corry, et al., 2005; Gillespie, 2008; Nonner, et al., 2000; Vora, et al., 2005; Yang, et al., 2004) It has been suggested, for example, that the electrostatic interactions that bind Ca^{2+} and Na^+ differently (Corry, et al., 2001; Corry and Chung, 2006) or the simple competition between differently charged ions for a limited space (Nonner, et al., 2000) can be enough to explain the different behaviours of sodium and calcium channels, but these ideas are yet to be tested in models containing atomic detail. Experimental studies have shown that eukaryotic calcium channels are continually occupied by at least one Ca^{2+} that guards against permeation of other ions. (Hess and Tsien, 1984)

How NavAb distinguishes between Na^+ and Ca^{2+} has not yet been explained, and this manuscript aims to address this issue. Na^+ currents are more than 20 times greater than Ca^{2+} currents in NavAb when measured without the other ion present. (Payandeh, et al., 2011) Reversal potentials of the closely related NachBac and NavSp1 channels measured in asymmetric solutions show a preference for Na^+ over Ca^{2+} of 7-15 (Shaya, et al., 2011; Yue, et al., 2002). These two ions are very similar in size, yet differ in charge, and so the mechanism of selectivity must rely of the consequences of this charge difference. Further confusing this issue is that a ring of four glutamate residues has been found to be essential to create Ca^{2+} over Na^+ selectivity in calcium channels, so one can ask why the presence of the ring of glutamates present in the bacterial sodium channels does not yield Ca^{2+} selectivity. Here we employ the recent structural information in molecular dynamics simulations to try to understand why the passage of Na^+ is preferred over Ca^{2+} in the bacterial voltage-gated sodium channel NavAB.

Materials and Methods:

Protein coordinates were obtained from the protein database, PDB accession code 3RVY. (Payandeh, et al., 2011) Only the pore forming region from residue 115 to 221 was included in the simulations. In order to conduct the molecular dynamics simulations, the protein was placed in a pre-equilibrated POPC lipid bilayer, solvated in a 72 x 72 x 82 Å box of TIP3P water with 250 mM NaCl, yielding a system with approximately 41,000 atoms as depicted in Figure 1. The protein was initially held fixed while the lipid and water were allowed to equilibrate for 2 ns, before the protein alpha carbons were restrained with a harmonic potential of force constant decreasing from 10 to 0.01 kcal/mol in 8 steps each lasting 1 ns. To account for the lipid molecules protruding into the centre of the pore in the crystal structure, the tails of four lipid molecules were restrained to the crystallographic positions with a force constant slowly increasing during the period in which the protein was restrained. During data collection they were restrained with a force constant of 0.1 kcal/mol/Å^2. A final 15 ns of equilibration were conducted at the final restraint values. In longer unrestrained simulations not described here, lipid remains constantly present in the lateral phenestrations. For the simulations involving Ca^{2+}, one Na^+ was replaced with Ca^{2+} and an additional Cl^- added to neutralise the system.

Potentials of mean force (PMF) were calculated using umbrella sampling. (Torrie and Valleau, 1974) To ensure other ions did not enter the selectivity filter during these simulations, all other ions were kept out of a sphere of radius 13 Å centred on the middle of the selectivity filter using harmonic repulsive potential with force constant 40 kcal/mol/Å^2. When making 1 ion PMFs, the axial separation (z) of the ion of interest and the centre of mass of the alpha carbons of the selectivity filter (residues 175-178) was restrained in 0.25 Å steps in the z-direction with a force constant of 12 kcal/mol/Å^2. For the two ion PMFs a force constant of 7 kcal/mol/Å^2 and 0.5 Å steps were employed. Simulations lasting 2ns were conducted at each window, with the first ns regarded as equilibration time and analysis conducted on only the second ns. Thus each single ion PMF involves 101 simulations for a total of 202 ns. The 2 ion Ca^{2+}/Na^+ PMF involves 695 simulations for a total of 1390 ns. To reduce the amount of equilibration time required in each umbrella window, a number of starting coordinates were generated in which one or two ions were swapped with equilibrated water molecules throughout the length of the pore. In the two ion case, this meant starting coordinates were generated with the ions separated by integer numbers of water molecules. Collective analysis was made with the weighted histogram analysis method (Kumar, et al., 1992) using the implementation of Grossfield. (Grossfield) The axial coordinate used in all the graphs is zeroed at the position of the centre of mass of the alpha carbons of the selectivity filter. The single Ca^{2+} PMF was obtained three times from three independent sets of simulations to gain an idea of the reproducibility of the results.

Unless otherwise stated, all simulations employed the CHARMM27 force field with CMAP correction for the protein and Ca^{2+},(MacKerell, et al., 1998) CHARMM36 for lipids,(Klauda, et al., 2010) and Na^+ and Cl^- parameters from Joung.(Joung and Cheatham, 2008) Because of the uncertainties involved in using a non-polarisable force field to describe interactions with Ca^{2+}, care should be taken not to overemphasise quantitative results involving this ion. Simulations were conducted with NAMD (Phillips, et al., 2005) with periodic boundary conditions using the particle mesh Ewald scheme for calculating electrostatic interactions, a 1 fs time-step at constant pressure (1 atm) and temperature (298K) (NPT ensemble). A harmonic potential of 0.01 kcal/mol/Å^2 was held on the alpha-carbon atoms, except for those forming the selectivity filter (residues 174 – 183) during data production. Coordination numbers were defined as the number of non-hydrogen atoms within 3.0 Å of the ion, the approximate position of the first minimum in the bulk ion-water oxygen radial distribution function.

To calculate the dehydration energies of the ions, we used the method of alchemical free energy perturbation (FEP) following the approach previously taken to examine partial dehydration of monovalent ions.(Song and Corry, 2009) To create a dehydration scenario similar to that for ions entering the channel, we first generated a water sphere of radius 15 Å with the test ion fixed at the center to represent the bulk solution. Beside this (20 Å from the center of the large sphere) we placed a smaller water sphere of radius 3.2 Å that contained the desired number of water molecules. Large constraints (100 kcal/mol Å^2) were applied to keep all of the atoms in the constant-volume spheres, as was done previously (Thomas, et al., 2007). Then, alchemical FEP calculations were performed for these systems in which the test ion was moved from the bulk-water sphere to the small water cluster, replacing a water molecule that was moved in the opposite direction. All simulation parameters except for the force field parameters for Na^+ and Ca^{2+} are the same as our previous study.(Song and Corry, 2009) To calculate the cost of removing water beyond the second solvation shell a similar procedure was conducted except, the small sphere had a radius of 6 Å and contained 32 water molecules, the average number found within the first and second solvation shells for both ions in bulk simulations. Each FEP calculation was repeated 9 times and the results show the average free energy change and the standard error in the mean.

Results:

The single ion PMFs for Na^+ and Ca^{2+} depicted in Figure 2 show that both ions are attracted from bulk (at the right side of the figure) into the selectivity filter of the channel and have an energy minimum adjacent to the ring of Glu177 residues at around z=5 Å In this position each ion is directly coordinated by the side chains of one glutamate residue as well as that of Ser178 as depicted in Figures 3A and C and evident in a plot of ion coordination numbers (Fig 4). Ca^{2+}binds more strongly to the protein than Na^+ as evidenced by the greater difference in the free energy of the binding site relative to bulk. Unlike in previous MD studies of a model pore containing four glutamate residues in which the Ca^{2+}binds centrally coordinated by multiple carboxylate groups (Yang, et al., 2004), here the ion directly coordinates to only one glu side chain. Part of the reason for this is likely to be that each of the glu side chains is held in position by hydrogen bonds to Ser 1180 and Met 1181 on the helix further from the pore.

To pass further into the pore, an ion must leave the embrace of the glutamate side chains. We have previously suggested that it is the unfavourable location where the ion passes through the plane of these side chains at which selectivity for Na^+ over K^+ arises.(Corry and Thomas, 2012) As for Na^+ and K^+, Ca^{2+} experiences an energy barrier at this position.

In contrast to both Na^+ and K^+, Ca^{2+} experiences a large energy barrier further into the pore, at around z=0.5 Å in Figure 2, which it must overcome to enter the central cavity of the pore. The size of the maximum energy barrier seen by each ion type ($Na^+ < K^+ < Ca^{2+}$) is in accord with the magnitude of current measured for each ion ($Na^+ > K^+ > Ca^{2+}$).(Payandeh, et al., 2011) The energy change for an ion to move from the energy minimum in the filter to the start of the central cavity is about 1 kcal/mol for Na^+ and 3 kcal/mol for Ca^{2+}, reinforcing that Ca^{2+} binds more strongly in the filter than Na^+. The single Ca^{2+} PMF was obtained 3 times from 3 independent sets of simulations to gain an appreciation of the reproducibility of the results. In all cases the maximum barrier for Ca^{2+} permeation occurs at the same location near z=0.5 Å.

To conduct our simulations we use the ‘pre-open’ structure of the channel, in which the selectivity filter is believed to be in an open state, but the activation gate is closed at the intracellular end of the pore.(Payandeh, et al., 2011) As a consequence, a large increase in free energy is seen at the left hand end of the PMFs shown in Figure 2 where the ion approaches the closed gate, and energy values in this region cannot be expected to represent those in a fully open channel. While it is possible that the closed gate could alter the energy profiles in the filter, we expect that the water filled cavity to largely screen the effect of the gate on the energy values in the filter.

To understand the reason for the large energetic barrier seen by Ca^{2+}, we show a snapshot of either Na^+ or Ca^{2+} in this position in Figures 3B and D. Here, the ion has moved beyond the Glu177 side chains, but not so far into the pore as to be surrounded by the backbone carbonyls of Thr175 and Leu176 which have been suggested to form an ideal environment for a solvated ion.(Payandeh, et al., 2011) Rather, the ion is surrounded by 5 or 6 water molecules which can only form limited interactions with the protein. Inspection of the coordination numbers of the ions in Fig. 4 shows that Na^+ maintains a coordination number close to 6 as it passes through this part of the pore, and begins to form occasional contacts with the backbone carbonyl groups. The coordination number of Ca^{2+}, however, shows 2 regions at which it drops below the average value of 7. When adjacent to the Glu177 residues, the coordination number begins to drop (labelled ① in the figure), but the strong interaction with the charged residues means this remains a favourable location for the ion. There is another significant drop at the location of the energy barrier (labelled ②) to a value less than 6.5.

In Table 1, we show the energetic cost of removing water from the hydration shell of Na^{+} and Ca^{2+} to see if this can account for the energy barriers seen in our PMFs. For Na^{+}, the penalty for removing a single water from the inner hydration shell costs ~3 kcal/mol. In contrast, Ca^{2+} holds on to both its inner and outer solvation shells much more strongly due to the increased electrostatic interactions of this ion with water molecules. From Table 1 it can be seen that removing one water molecule from the inner shell of Ca^{2+} (going from a coordination number of 7 to 6) has an energy cost of ~ 8 kcal/mol. This suggests that removal of (on average) half a water molecule from the solvation shell could account for half the energy barrier seen by Ca^{2+}. The results in table also show that Ca^{2+} is sensitive to the environment outside the immediate coordination shell and so it is plausible that changes in the first solvation shell and limited interactions with more distant water could account for the barrier seen in our PMFs.

To further support our claim that the differences in coordination numbers can account for the different free energy barriers seen by the ions in the channel, we plot the average ion-water and ion-protein interaction energy as a function of ion position for Ca^{2+} in the selectivity filter in Figure 5A. The ion-protein and ion-water interactions are almost mirror images of one another. It can be seen that a strong attractive interaction between the ion and protein arises when the ion is close to the ring of Glu177 residues (z=5 Å). At this point, the replacement of water in the coordination shell with protein yields a less negative ion-water interaction. As the ion moves through the centre of the selectivity filter, the ion-protein interaction becomes less negative and the ion-water interaction more negative. In figure 5B we plot the sum of the ion-protein and ion-water interactions as either a single Na^{+} or Ca^{2+} moves through the pore (vertically shifted so the results for the two ions can be compared). The fact that the two interaction terms are almost mirror images means that the sum of the two produces a relatively flat line. While the sum of the interactions fluctuates as a function of ion position, it is much more stable for Na^{+} than for Ca^{2+}. At the location of the energy barrier for Ca^{2+} seen in the PMFs (z=0.5 Å), both ions see an upward deflection in the curve, indicating that the ion-protein interaction is not able to compensate for the reduced ion-water interaction that is enforced by the limited space in the pore. Reinforcing the conclusion drawn from the graph of coordination numbers, the barrier seen for Ca^{2+} seems to be due to a less than ideal combination of ion-protein and ion-water interactions. In other words, Ca^{2+} experiences a degree of dehydration which is not compensated by interactions with the protein. The second and further hydration shells are also held more strongly by Ca^{2+} than Na^{+}, and so their removal will also disfavour Ca^{2+} as this does not appear to be compensated by interactions with the protein.

Having described the differences in the permeation of a single Na^{+} and a single Ca^{2+} ion through the channel, we next turn our attention to what would occur if multiple ions are allowed to enter the pore. In Figure 6 we plot the PMF as a function of the position of two Na^{+} ions in the pore. This graph is generated from the same data presented in our previous work,(Corry and Thomas, 2012) and shows how the presence of two Na^+ ions can slightly reduce the barriers to ion conduction compared to the case when a single ion permeates on its own. The plot shows that one ion is likely to always occupy the binding site by the Glu177 residues and that conduction is most likely to occur when a second ion displaces the first ion from this position and pushes it through the pore in a loosely coupled knock on mechanism (ie following the dotted line from state 1 to 2 to 3 as shown in the insets to the figure). The maximum barrier for this process is approximately 2.5 kcal/mol.(Corry and Thomas, 2012) Figure 6 also shows that it is possible for a Na^+ ion to bypass a resident ion (crossing the diagonal on the plot).The energy barrier for this process is only 2 kcal/mol greater than that seen for knock on conduction. Thus, ions may be able to pass each other in the pore and so conduction may not be a strictly single file process.

The PMF obtained with two Ca^{2+} ions in the channel is plotted in Figure 7. The barrier for Ca^{2+} conduction is lowered by the presence of the second ion, as can be seen by the reduced barrier to move along the path indicated by the dotted line compared to moving along the top edge of the figure. The maximum barrier for conduction drops from ~8kcal/mol in the single ion PMF to ~ 4.5 in the two ion case, more consistent with the observation that Ca^{2+} currents are 20 fold less than Na^+ currents. Thus, Ca^{2+} will also be expected to conduct in a knock on mechanism. The largest barrier to permeation is located at the same position as for the single ion PMF (z=0.5 Å), indicating that the analysis of the origin of this barrier is relevant in the case of multi-ion conduction. Figure 7 also indicates that Ca^{2+} ions are unlikely to pass each other in the pore.

In Figure 8 we show the PMF in a mixture of Ca^{2+} and Na^+. If we start with the Ca^{2+} adjacent to Glu177 (as depicted in inset 3) then we can see than the barrier for Ca^{2+} to move through the channel is no smaller with Na^+ nearby (moving from the state shown in inset 3 to inset 1) than if Ca^{2+} is moving on its own (state 3 to state 2). In each case the maximum barrier is ~ 6.5 kcal/mol, which is similar to that seen in the single ion Ca^{2+} PMF. The figure also shows the profile for Na^+ to bypass Ca^{2+} (ie moving along the dotted line from state 3 to 4 to 5 to 6). Here the maximum barrier of ~5 kcal/mol arises at the point at which the ions move past one another (between states 4 and 5). Thus, it is more likely for Na^+ to bypass Ca^{2+} than for Ca^{2+} to be pushed through the pore. Finally we can see that if Na^+ starts in the pore (state 5) then Ca^{2+} can easily displace it and push it through the pore (state 6).

Discussion:

In the absence of other cations, our simulations imply that the conduction of Na^+ is rapid due to the small energy barriers experienced by these moving through the pore in a sequential knock on process. In contrast, we see a much larger barrier for Ca^{2+} to pass, in accord with its lower current. The barrier for Ca^{2+} is slightly lower in the presence of Na+ and is further lowered in the presence of a second Ca^{2+}.

The results shown in Fig 6 and 8, however, also indicate that ions can pass each other inside the pore. When two Na^+ ions are in the pore (Fig 6) the barrier for ions passing each other is only a little larger than seen for knock on conduction, while Na^+ can pass K^+ with almost no additional barrier.(Corry and Thomas, 2012) If Ca^{2+} resides in the pore, the entry of a Na^+ ion does not increase the likelihood of the Ca^{2+}passing through the pore. Na^+ can also move around a resident Ca^{2+} ion and conduct through the pore, however the barrier for this process is larger than when only Na^+ is present. As a consequence, we would expect the presence of Ca^{2+} in the filter to attenuate Na^+ currents, but not to completely prevent them.

It has previously been shown that divalent cations interfere with the conduction of Na^+ in eukaryotic sodium channels. (French, et al., 1994; Mozhayeva, et al., 1982; Ravindran, et al., 1991; Tanguy and Yeh, 1988; Taylor, et al., 1976; Woodhull, 1973; Yamamoto, et al., 1984) But, in the bacterial channel NachBac, the presence of 1mM Ca^{2+} only slightly reduces Na^+ currents,(Ren, et al., 2001) This could only arise if either Ca^{2+} did not enter the pore or if Na^+ can pass Ca^{2+} ions resident in the pore. Our simulations results would suggest a larger attenuation of Na^+ currents in the presence of Ca^{2+} in NavAB than seen experimentally for NachBac. While it is possible that these channels are different in this respect, the sequence similarity of the two proteins makes this seem unlikely. The proximity of the four Glu177 residues makes it possible that one or more of these residues will be protonated as is suspected to be the case in calcium channels.(Corry, et al., 2001; Root and Mackinnon, 1994) Previously we suggested that the protonation of a single Glu side chain would not influence the selectivity of the channel for Na^+over K^+,(Corry and Thomas, 2012) however, this does reduce the strength of binding of the ion to the external site. The position of the saddle point in Figure 7 shows that the easiest way for Na^+ to pass a resident Ca^{2+} is for the Ca^{2+} ion to back slightly out of the binding site. Any reduction in affinity of the site would make it easier for a resident Ca^{2+} ion to do this. This, in turn, may expediate the passage of Na^+ past a resident Ca^{2+}, and thus limit the attenuation of Na^+ currents seen in the presence of Ca^{2+}.

Another important factor to consider is how accurately the classical simulations used here can be expected to reproduce the free energies of the transport process. Ideally, the ion parameters need to be able to reproduce the interactions of the ions with a range of molecules (including protein functional groups and water) as well as the structure and dynamics of interacting molecules, something which is difficult to achieve with classical non-polarisable models. Dealing with divalent ions is particularly difficult in non-polar force fields. Due their high charge density, divalent ions are more likely to polarise surrounding molecules than is the case for monovalent ions,(Bako, et al., 2002; Bucher and Kuyucak, 2008) an effect which is not considered in the present study. The parameters for Na^+ and K^+ have been shown to accurately reproduce a range of properties including hydration energies, the structures of ion-water clusters and crystals and binding energies.(Joung and Cheatham, 2008) The parameters for Ca^{2+} were also optimised to reproduce hydration free energies and binding energies with water, (Marchand and Roux, 1998) and have been used in a range of studies of biological molecules,(Cates, et al., 2002; Sotomayor and Schulten, 2008; Sotomayor, et al., 2012) but have not been tested as rigorously on specific interactions with protein functional groups or structural aspects. Despite these caveats, we believe that the general principles that yield strong binding of Ca^{2+} to the external binding site and the uncompensated energy cost of dehydration that yields the main energy barrier for Ca^{2+} in the pore, are likely arise even with a polarisable force field. However, caution should be applied to making quantitative predictions. It is certainly possible that the Ca^{2+} parameters influence the ease by which Na^+ can pass resident Ca^{2+} ions.

It is interesting to ponder how changes to NavAB could lead to Ca^{2+} selectivity. A small number of mutations have been shown to be able to convert bacterial sodium channels into being Ca^{2+} selective.(Shaya, et al., 2011; Yue, et al., 2002) These involve introducing additional acidic residues at the mouth of the channel, the presence of which seems to be essential for generating Ca^{2+} selectivity. The additional negative charge may increase the chance of a second Ca^{2+} entering the pore to yield knock on Ca^{2+} conduction. The PMF determined here with two Ca^{2+} in the pore suggests that the presence of multiple divalent ions can reduce the major barrier to Ca^{2+} seen in our simulations, but given that this barrier arises far from the location of the mutations further simulations will be required to shed light on this issue. The additional negative charge may also accentuate the difference in the binding affinity of the filter for Ca^{2+} compared to Na^{+}.

Given that Ca^{2+} binds more strongly than Na^{+}in NavAB, and experimental studies of eukaryotic calcium channels show they are permanently occupied by Ca^{2+},(Hess and Tsien, 1984) it is also possible that Ca^{2+} selectivity could be obtained by preventing Na^{+} from being able to pass a resident Ca^{2+} ion. Figure 8 indicates that such passing is likely to occur in the channel mouth, slightly external to Glu177. So, selectivity for Ca^{2+}over Na^{+} may also be achieved by narrowing the diameter of the pore entrance to create genuinely single file conduction. If such a narrowing took place external to Glu177, it need not significantly change the diameter of the narrow point of the selectivity filter and so could keep this consistent with experimental estimates of the minimum pore diameter in eukaryotic calcium channels (>5.5 Å). (Mccleskey and Almers, 1985) Similarly, if the Glu177 side chains were less constrained in position by hydrogen bonds to the rest of the protein, then it is possible that multiple side chains would coordinate a passing Ca^{2+} and occlude the pore as is studies of a model pore (Yang, et al., 2004). Site directed mutagenesis and electrophysiology has shown that in calcium channels the four glutamate residues are not symmetrically positioned (Ellinor, et al., 1995) and it is possible that this would also weaken the binding affinity of Ca^{2+} to the filter to allow conduction to occur more easily.

Conclusions:

In agreement with experimental data, the single and multi-ion free energy profiles calculated here indicate that the Ca^{2+} conductance of NavAb is likely to be much smaller than for Na^{+}. While the results presented here signify that the channel will prefer the conduction of Na^{+} in mixed solutions, the difference in energy barriers for the conduction of Na^{+} and Ca^{2+} in mixed solution are small, in agreement with permeability ratios in the order of 10:1.(Yue, et al., 2002) The reason that Ca^{2+} has difficulty in passing through the pore appears to be due to the limited space midway through the selectivity filter between the sections lined by the Glu177 side chains and the carbonyl backbones of Leu176. The lack of both space and polar groups here limits ion coordination numbers without offering compensating ion-protein interactions. Ca^{2+} suffers a more significant drop in coordination numbers at this point and thus a larger dehydration penalty than does Na^{+}. Our results indicate that ions can pass each other in the pore, which is why Ca^{2+} does not block Na^{+} currents, however our data does predict a larger attenuation of Na^{+} currents by Ca^{2+} than was seen in the related channel NachBac.

Acknowledgements:

Michael Thomas is thanked for helpful discussions.

Figure Legends:

Figure 1: Simulation system. A cross section of the simulation system is shown, with two of the four protein chains shown in purple, lipid in brown, Na^+ in yellow, Cl^- in green and the volume sampled by water molecules indicated by the transparent surface.

Figure 2: Single ion potential of mean force (PMF) for Na^+ (blue), Ca^{2+} (red) and K^+ (black dashed line) is shown as a function of the axial position of the ion, zeroed at the centre of the selectivity filter. The ion is in bulk water at the right side of the graph and in the central cavity of the channel on the left hand side. For Ca^{2+} the PMF shown is the average of 3 independent sets of simulations, with the standard deviation in the three values shown shaded in pink.

Figure 3: Simulation snapshots showing the ion and coordinating water when either Na^+ (A) or Ca^{2+} (C) is at the external binding site, or when the Na^+(B) and Ca^{2+} (D) is at the location of the largest barrier experienced by Ca^{2+}.

Figure 4: Coordination numbers for (A) Na^+ and (B) Ca^{2+} as a function of the axial position of the ion in the pore. The total coordination number is shown in black, while the contribution from water (blue), glutamate side chains (red) and other protein residues (green) are indicated. Standard errors in the mean are smaller than the data points and are not shown.

Figure 5: Ion-water and ion-protein interaction energies. (A) the Ca^{2+}-protein (black) and Ca^{2+}-water (blue) interaction is plotted as a function of the axial position of the ion in the pore. (B) The sum of the ion-water and ion-protein interaction energies is shown for both Na^+ (blue) and Ca^{2+} (red) as a function of the axial position of the ion in the pore. As only changes in the total energy with position are important for the discussion presented, the curves on B have been vertically shifted to zero at the left hand side to allow for the results for Ca^{2+} and Na^+ to be more easily compared.

Figure 6: Two ion potential of mean force for Na^+. The PMF is plotted as a function of the positions of two Na^+ ions in the pore. Contours are at 1 kcal/mol intervals. Representative snapshots are shown in the insets for three low energy configurations, whose locations are shown on the plot. The approximate lowest energy pathway for ion permeation is shown by the dotted line.

Figure 7: Two ion potential of mean force for Ca^{2+}. The PMF is plotted as a function of the positions of two Ca^{2+} ions in the pore. Contours are at 1 kcal/mol intervals. Representative snapshots are shown in the insets for four low energy configurations, whose locations are shown on the plot. The approximate lowest energy pathway for ion permeation is shown by

the dotted line. A smaller range of coordinates is shown compared to the other two ion PMFs as the ions are unlikely to pass each other in the pore.

Figure 8: Mixed ion potential of mean force. The PMF is plotted as a function of the position of one Ca^{2+} ion (x-axis) and one Na^+ ion (y-axis). Contours are at 1 kcal/mol intervals. Representative snapshots are shown in the insets for six low energy configurations whose locations are shown on the plot. The approximate lowest energy pathway for Na^+ to permeate through the pore by passing a resident Ca^{2+} ion is shown by the dotted line.

References:

Bako, I., Hutter, J. and Palinkas, G. (2002) Car-Parrinello molecular dynamics simulation of the hydrated calcium ion, *J Chem Phys*, **117**, 9838-9843.
Boda, D., *et al.* (2009) Ionic selectivity in L-type calcium channels by electrostatics and hard-core repulsion, *J Gen Physiol*, **133**, 497-509.
Bucher, D. and Kuyucak, S. (2008) Polarization of water in the first hydration shell of K+ and Ca2+ ions, *J Phys Chem B*, **112**, 10786-10790.
Cates, M.S., Teodoro, M.L. and Phillips, G.N. (2002) Molecular mechanisms of calcium and magnesium binding to parvalbumin, *Biophys J*, **82**, 1133-1146.
Catterall, W.A. (2000) From ionic currents to molecular mechanisms: The structure and function of voltage-gated sodium channels, *Neuron*, **26**, 13-25.
Cibulsky, S.M. and Sather, W.A. (2000) The EEEE locus is the sole high-affinity Ca2+ binding structure in the pore of a voltage-gated Ca2+ channel - Block by Ca2+ entering from the intracellular pore entrance, *J Gen Physiol*, **116**, 349-362.
Corry, B., *et al.* (2000) A model of calcium channels, *Bba-Biomembranes*, **1509**, 1-6.
Corry, B., *et al.* (2001) Mechanisms of permeation and selectivity in calcium channels, *Biophys J*, **80**, 195-214.
Corry, B. and Chung, S.H. (2006) Mechanisms of valence selectivity in biological ion channels, *Cell Mol Life Sci*, **63**, 301-315.
Corry, B. and Thomas, M. (2012) Mechanism of ion permeation and selectivity in a voltage gated sodium channel, *J Am Chem Soc*, **134**, 1840-1846.
Corry, B., Vora, T. and Chung, S.H. (2005) Electrostatic basis of valence selectivity in cationic channels, *Bba-Biomembranes*, **1711**, 72-86.
Ellinor, P.T., *et al.* (1995) Ca2+ Channel Selectivity at a Single-Locus for High-Affinity Ca2+ Interactions, *Neuron*, **15**, 1121-1132.
Favre, I., Moczydlowski, E. and Schild, L. (1996) On the structural basis for ionic selectivity among Na+, K+, and Ca2+ in the voltage-gated sodium channel, *Biophys J*, **71**, 3110-3125.
French, R.J., *et al.* (1994) Ion Permeation, Divalent Ion Block, and Chemical Modification of Single Sodium-Channels - Description by Single-Occupancy and Double-Occupancy Rate-Theory Models, *J Gen Physiol*, **103**, 447-470.
Furini, S. and Domene, C. (2012) On Conduction in a Bacterial Sodium Channel, *Plos Comput Biol*, **8**.
Gillespie, D. (2008) Energetics of divalent selectivity in a calcium channel: The ryanodine receptor case study, *Biophys J*, **94**, 1169-1184.
Goldin, A.L. (2001) Resurgence of sodium channel research, *Annu Rev Physiol*, **63**, 871-894.
Grossfield, A. An implementation of WHAM: the Weighted Histogram Analysis Method. http://membrane.urmc.rochester.edu/Software/WHAM/WHAM.html (accessed 26/1/2010).
Heinemann, S.H., *et al.* (1992) Calcium-Channel Characteristics Conferred on the Sodium-Channel by Single Mutations, *Nature*, **356**, 441-443.
Hess, P. and Tsien, R.W. (1984) Mechanism of Ion Permeation through Calcium Channels, *Nature*, **309**, 453-456.

Hille, B. (2001) *Ion channels of excitable membranes*. Sinauer, Sunderland, Mass.
Joung, I.S. and Cheatham, T.E. (2008) Determination of alkali and halide monovalent ion parameters for use in explicitly solvated biomolecular simulations, *J Phys Chem B*, **112**, 9020-9041.
Klauda, J.B.*, et al.* (2010) Update of the CHARMM All-Atom Additive Force Field for Lipids: Validation on Six Lipid Types, *J Phys Chem B*, **114**, 7830-7843.
Kumar, S.*, et al.* (1992) The Weighted Histogram Analysis Method for Free-Energy Calculations on Biomolecules .1. The Method, *J Comput Chem*, **13**, 1011-1021.
MacKerell, A.D.*, et al.* (1998) All-atom empirical potential for molecular modeling and dynamics studies of proteins, *J Phys Chem B*, **102**, 3586-3616.
Marchand, S. and Roux, B. (1998) Molecular dynamics study of calbindin D-9k in the apo and singly and doubly calcium-loaded states, *Proteins*, **33**, 265-284.
Mccleskey, E.W. and Almers, W. (1985) The Ca Channel in Skeletal-Muscle Is a Large Pore, *P Natl Acad Sci USA*, **82**, 7149-7153.
McCusker, E.C.*, et al.* (2012) Structure of a bacterial voltage-gated sodium channel pore reveals mechanisms of opening and closing, *Nat Commun*, **3**, 1102.
Mozhayeva, G.N., Naumov, A.P. and Khodorov, B.I. (1982) Potential-Dependent Blockage of Batrachotoxin-Modified Sodium-Channels in Frog Node of Ranvier by Calcium-Ions, *Gen Physiol Biophys*, **1**, 281-282.
Nonner, W., Catacuzzeno, L. and Eisenberg, B. (2000) Binding and selectivity in L-type calcium channels: A mean spherical approximation, *Biophys J*, **79**, 1976-1992.
Payandeh, J.*, et al.* (2012) Crystal structure of a voltage-gated sodium channel in two potentially inactivated states, *Nature*, **486**, 135-U166.
Payandeh, J.*, et al.* (2011) The crystal structure of a voltage-gated sodium channel, *Nature*, **475**, 353-U104.
Phillips, J.C.*, et al.* (2005) Scalable molecular dynamics with NAMD, *J Comput Chem*, **26**, 1781-1802.
Ravindran, A., Schild, L. and Moczydlowski, E. (1991) Divalent-Cation Selectivity for External Block of Voltage-Dependent Na+ Channels Prolonged by Batrachotoxin - Zn2+ Induces Discrete Substates in Cardiac Na+ Channels, *J Gen Physiol*, **97**, 89-115.
Ren, D.J.*, et al.* (2001) A prokaryotic voltage-gated sodium channel, *Science*, **294**, 2372-2375.
Root, M.J. and Mackinnon, R. (1994) 2 Identical Noninteracting Sites in an Ion-Channel Revealed by Proton-Transfer, *Science*, **265**, 1852-1856.
Shaya, D.*, et al.* (2011) Voltage-gated sodium channel (Na-V) protein dissection creates a set of functional pore-only proteins, *P Natl Acad Sci USA*, **108**, 12313-12318.
Song, C. and Corry, B. (2009) Intrinsic Ion Selectivity of Narrow Hydrophobic Pores, *J Phys Chem B*, **113**, 7642-7649.
Sotomayor, M. and Schulten, K. (2008) The allosteric role of the Ca(2+) switch in adhesion and elasticity of C-cadherin, *Biophys J*, **94**, 4621-4633.
Sotomayor, M.*, et al.* (2012) Structure of a force-conveying cadherin bond essential for inner-ear mechanotransduction, *Nature*, **492**, 128-+.
Sun, Y.M.*, et al.* (1997) On the structural basis for size-selective permeation of organic cations through the voltage-gated sodium channel - Effect of alanine mutations at the DEKA locus on selectivity, inhibition by Ca2+ and H+, and molecular sieving, *J Gen Physiol*, **110**, 693-715.
Tang, S.*, et al.* (1993) Molecular Localization Studies of the Dihydropyridine (Dhp) Binding-Site in the Cardiac L-Type Voltage Dependent Ca-2+ Channel (L-Vdcc) Alpha-1 Subunit Reveal Motif Iv S3 to Iv S6 as Essential, *Biophys J*, **64**, A6-A6.
Tanguy, J. and Yeh, J.Z. (1988) Divalent-Cation Block of Normal and Btx-Modified Sodium-Channels in Squid Axons, *Biophys J*, **53**, A229-A229.
Taylor, R.E., Armstrong, C.M. and Bezanilla, F. (1976) Block of Sodium Channels by External Calcium-Ions, *Biophys J*, **16**, A27-A27.
Thomas, M., Jayatilaka, D. and Corry, B. (2007) The predominant role of coordination number in potassium channel selectivity, *Biophys J*, **93**, 2635-2643.

Torrie, G.M. and Valleau, J.P. (1974) Monte-Carlo Free-Energy Estimates Using Non-Boltzmann Sampling - Application to Subcritical Lennard-Jones Fluid, *Chem Phys Lett*, **28**, 578-581.
Vora, T., Corry, B. and Chung, S.H. (2005) A model of sodium channels, *Bba-Biomembranes*, **1668**, 106-116.
Woodhull, A.M. (1973) Ionic Blockage of Sodium Channels in Nerve, *J Gen Physiol*, **61**, 687-708.
Yamamoto, D., Yeh, J.Z. and Narahashi, T. (1984) Voltage-Dependent Calcium Block of Normal and Tetramethrin-Modified Single Sodium-Channels, *Biophys J*, **45**, 337-344.
Yang, Y., Henderson, D. and Busath, D.D. (2004) Calcium block of sodium current in a model calcium channel: Cylindrical atomistic pore with glutamate side chains, *Mol Simulat*, **30**, 75-80.
Yue, L.X.*, et al.* (2002) The cation selectivity filter of the bacterial sodium channel, NaChBac, *J Gen Physiol*, **120**, 845-853.
Zhang, X.*, et al.* (2012) Crystal structure of an orthologue of the NaChBac voltage-gated sodium channel, *Nature*, **486**, 130-U160.

Figure 1

Simulation system

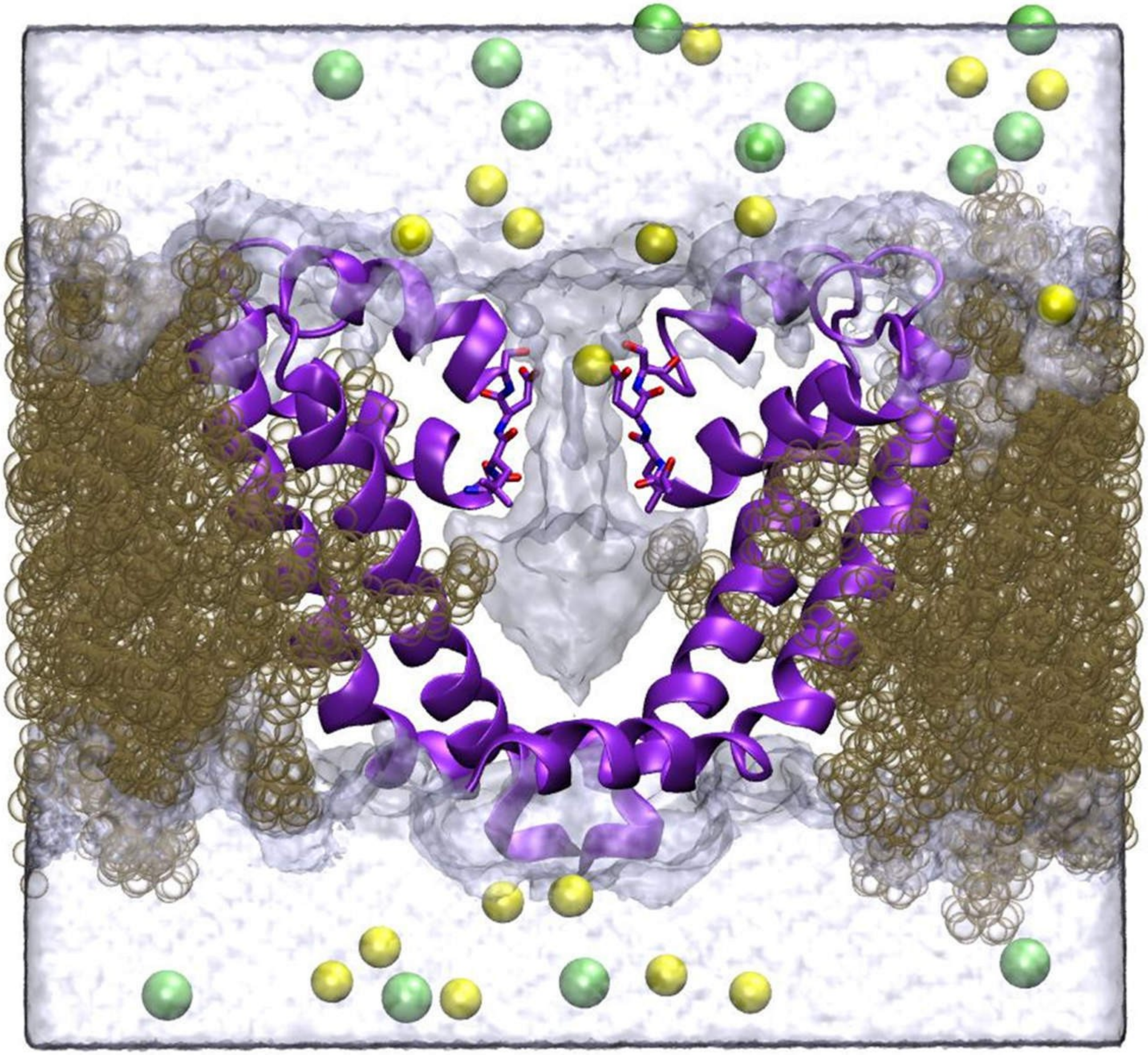

Figure 2

Single ion potential of mean force

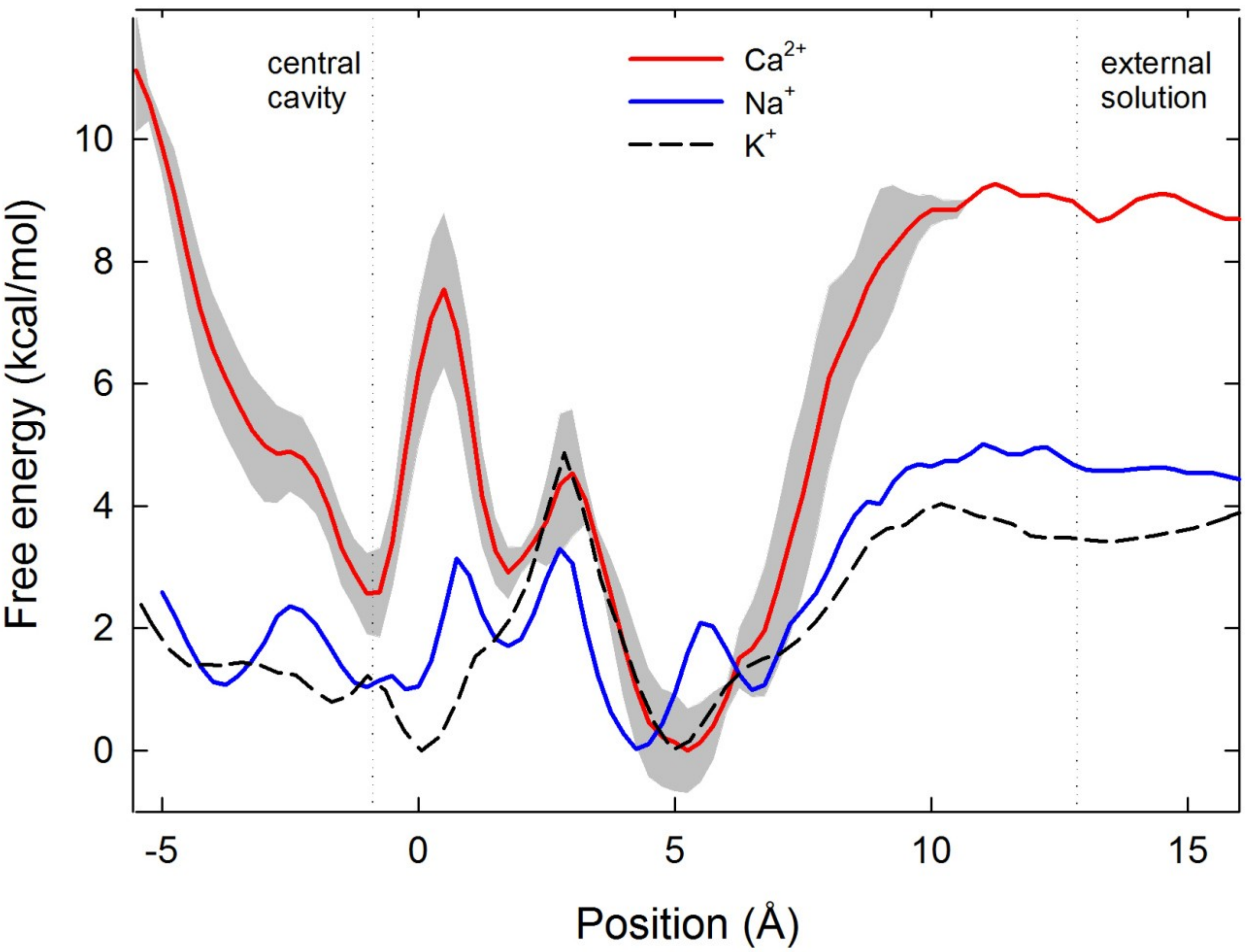

Figure 3

Snapshots of ions in the channel

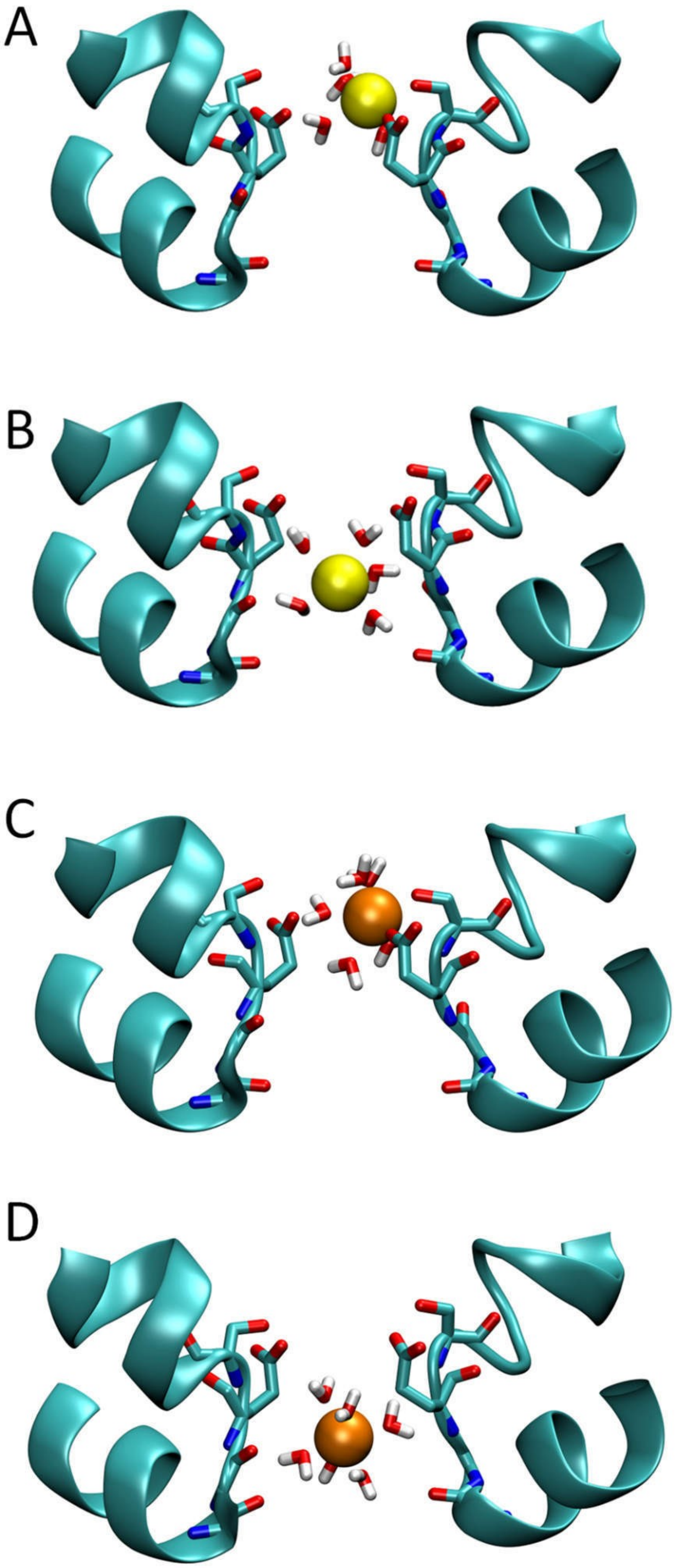
A
B
C
D

Figure 4

Coordination numbers of ions in the channel

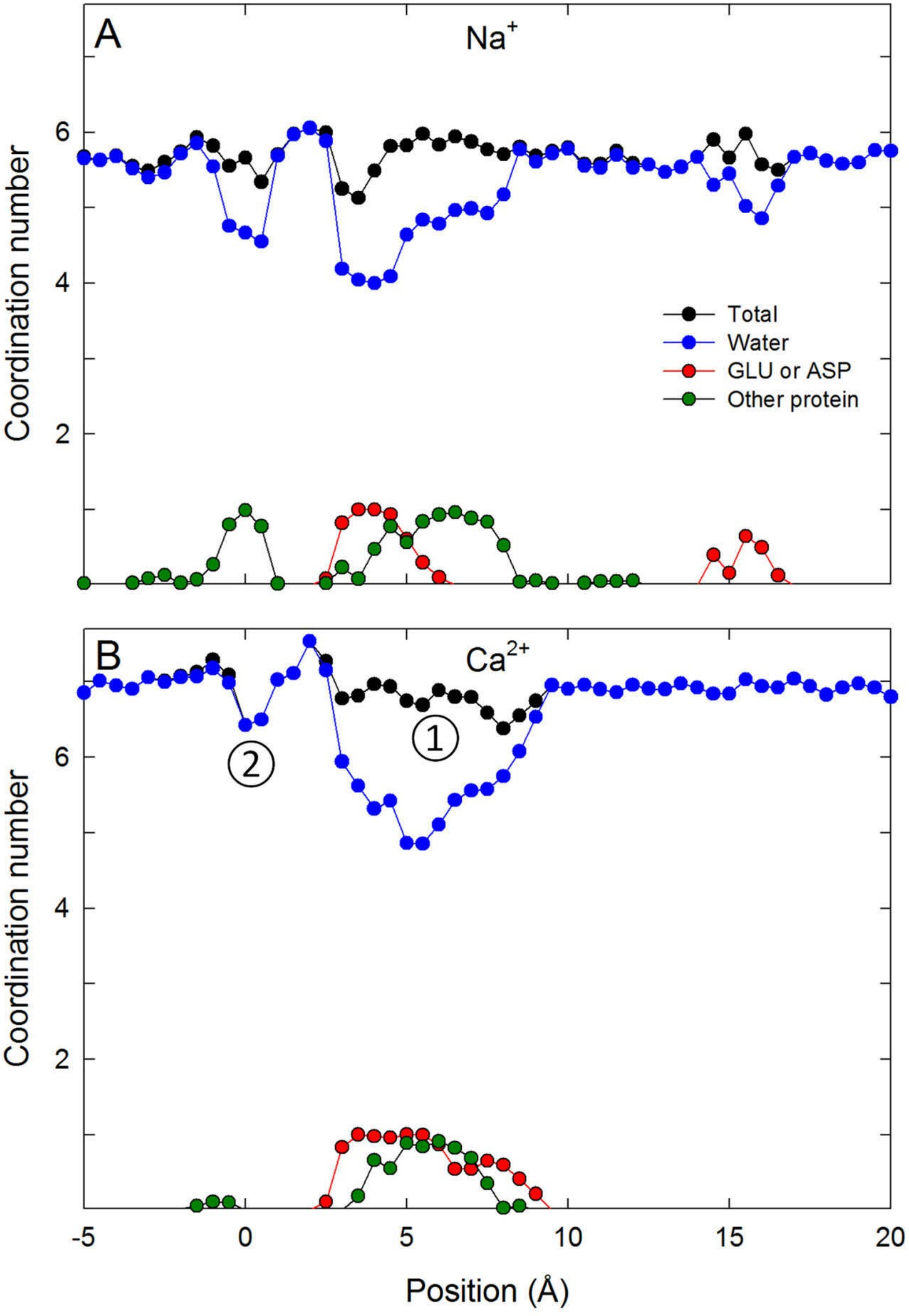
A
Na$^+$
Coordination number
6
4
2
Total
Water
GLU or ASP
Other protein
B
Ca^{2+}
①
②
Coordination number
6
4
2
-5
0
5
10
15
20
Position (Å)

Figure 5

Interaction energies of the ions with water and protein when in the channel

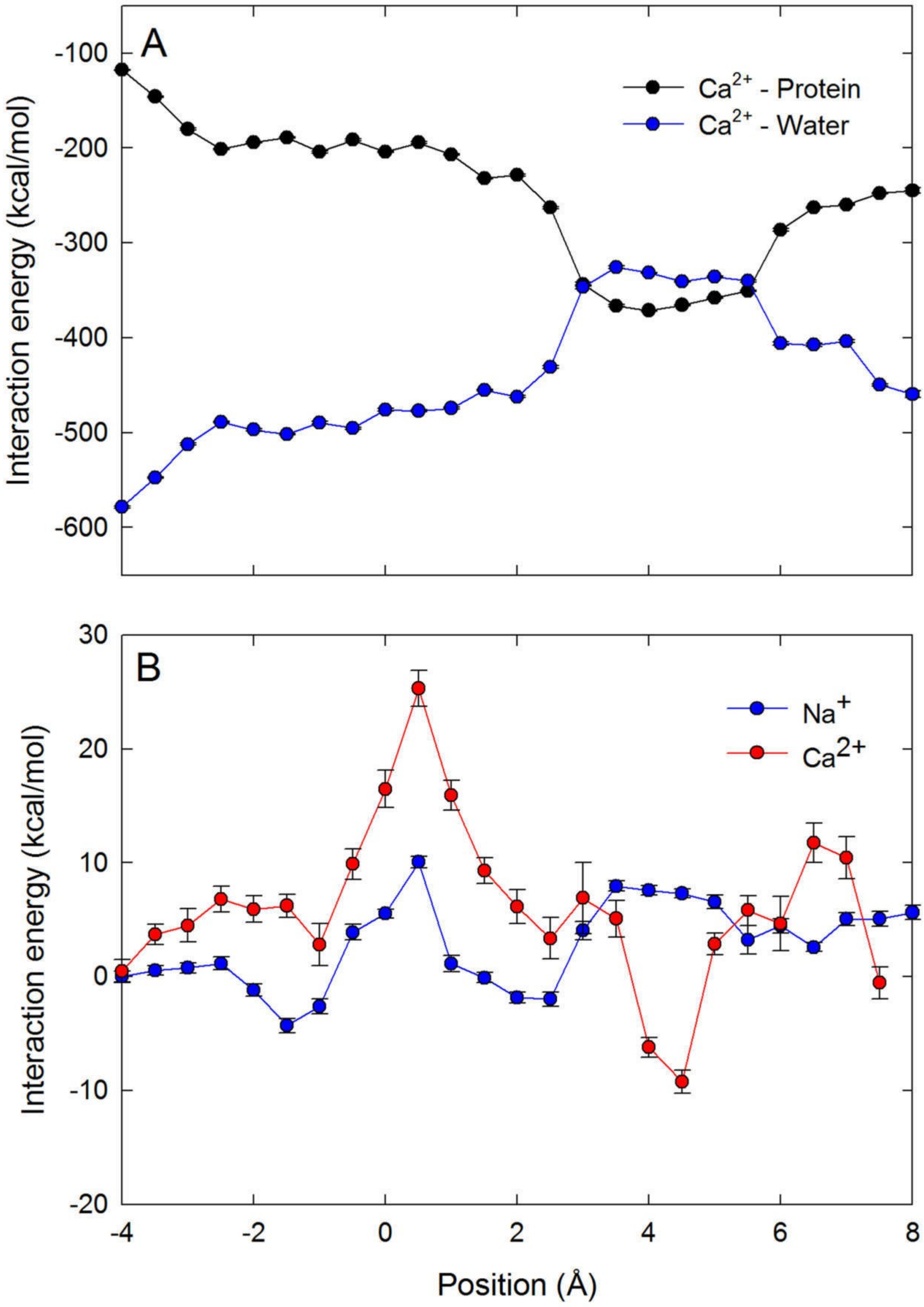
A
Ca²⁺ - Protein
Ca²⁺ - Water
Interaction energy (kcal/mol)
-100
-200
-300
-400
-500
-600
B
Na⁺
Ca²⁺
Interaction energy (kcal/mol)
30
20
10
0
-10
-20
-4
-2
0
2
4
6
8
Position (Å)

Figure 6

Potential of mean force for two sodium ions in the channel

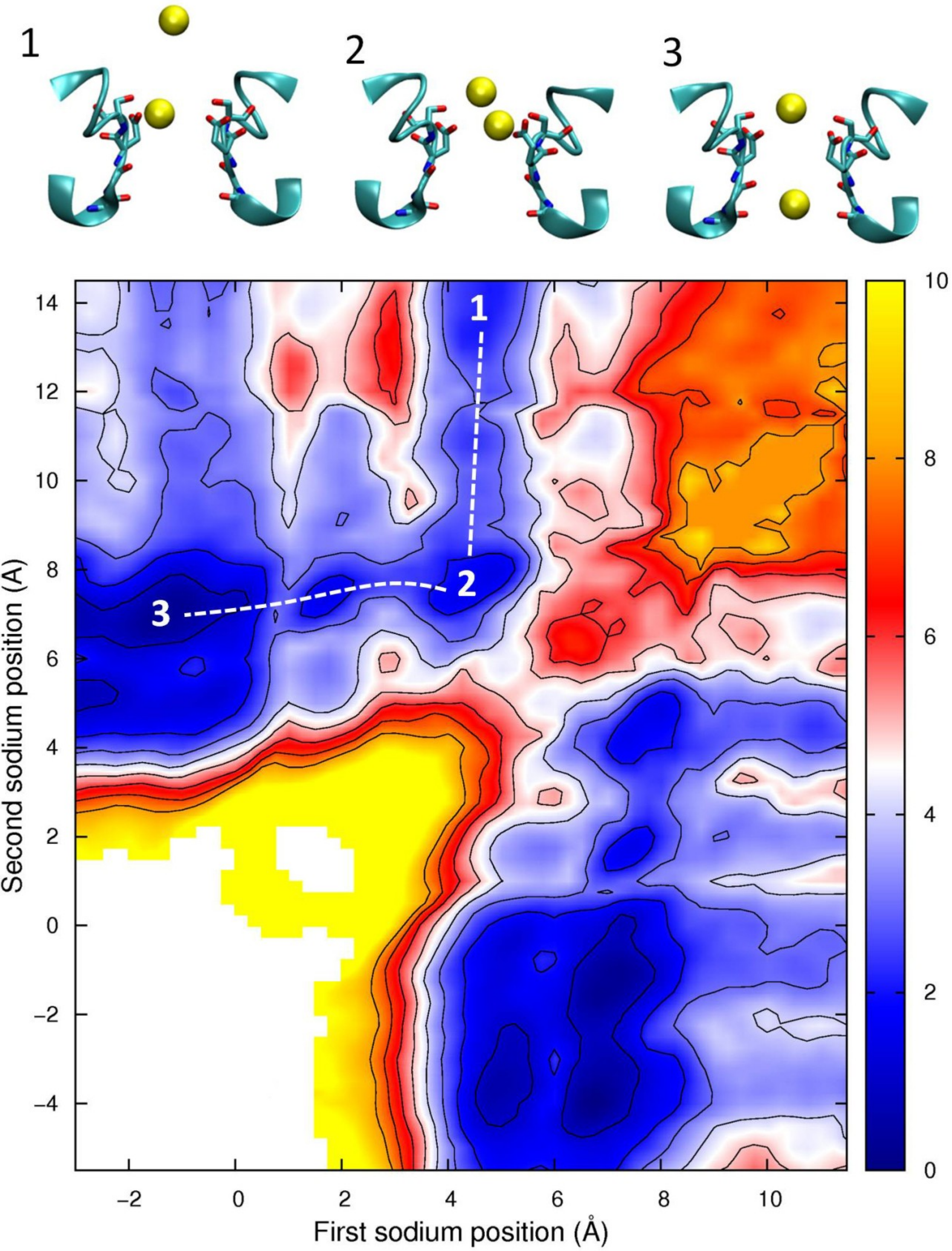
1
2
3
1
2
3
14
12
10
8
6
4
2
0
−2
−4
−2
0
2
4
6
8
10
Second sodium position (Å)
First sodium position (Å)
10
8
6
4
2
0

Figure 7

Potential of mean force for two calcium ions in the channel

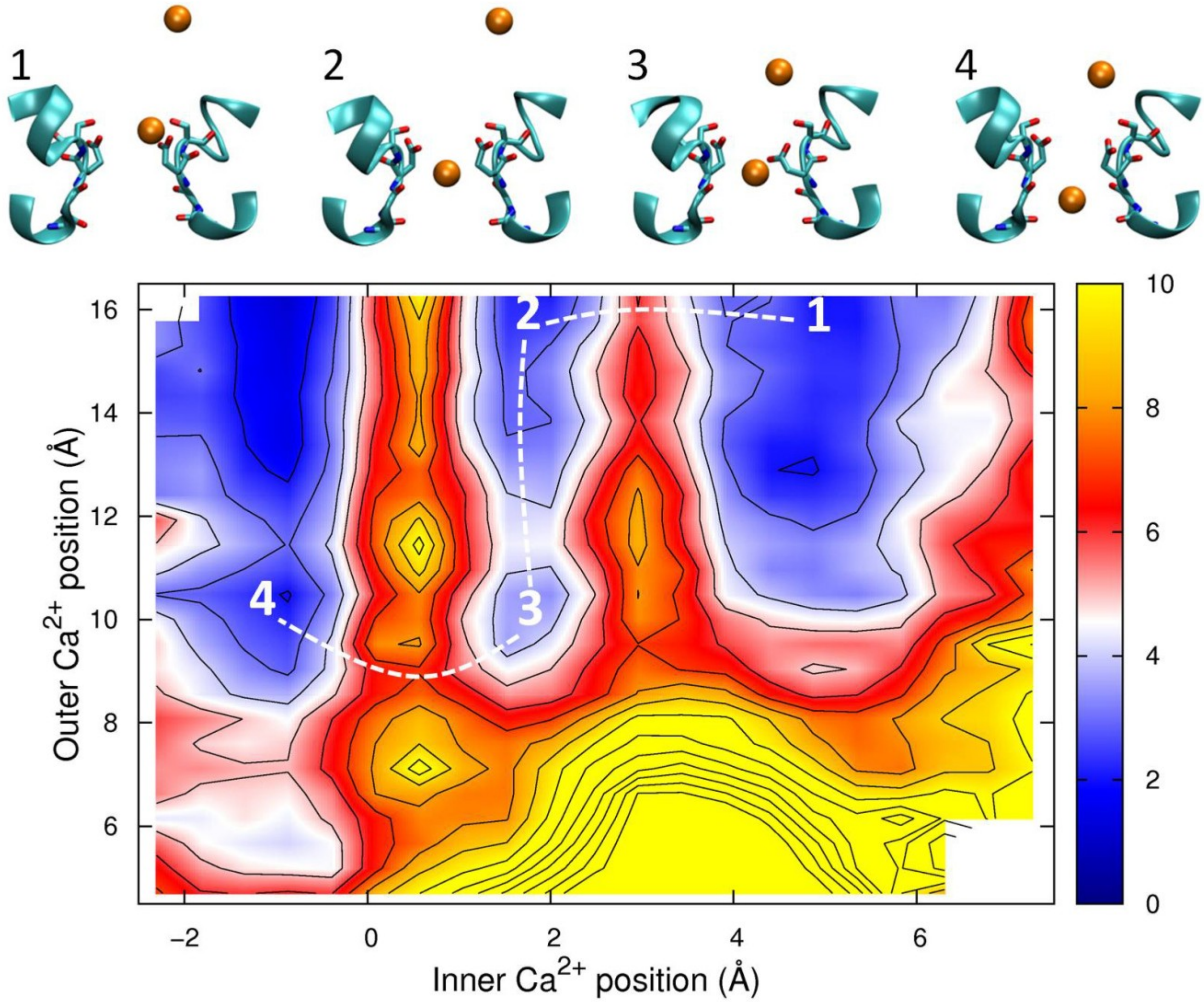

Figure 8

Potential of mean force for one calcium and one sodium ion in the channel

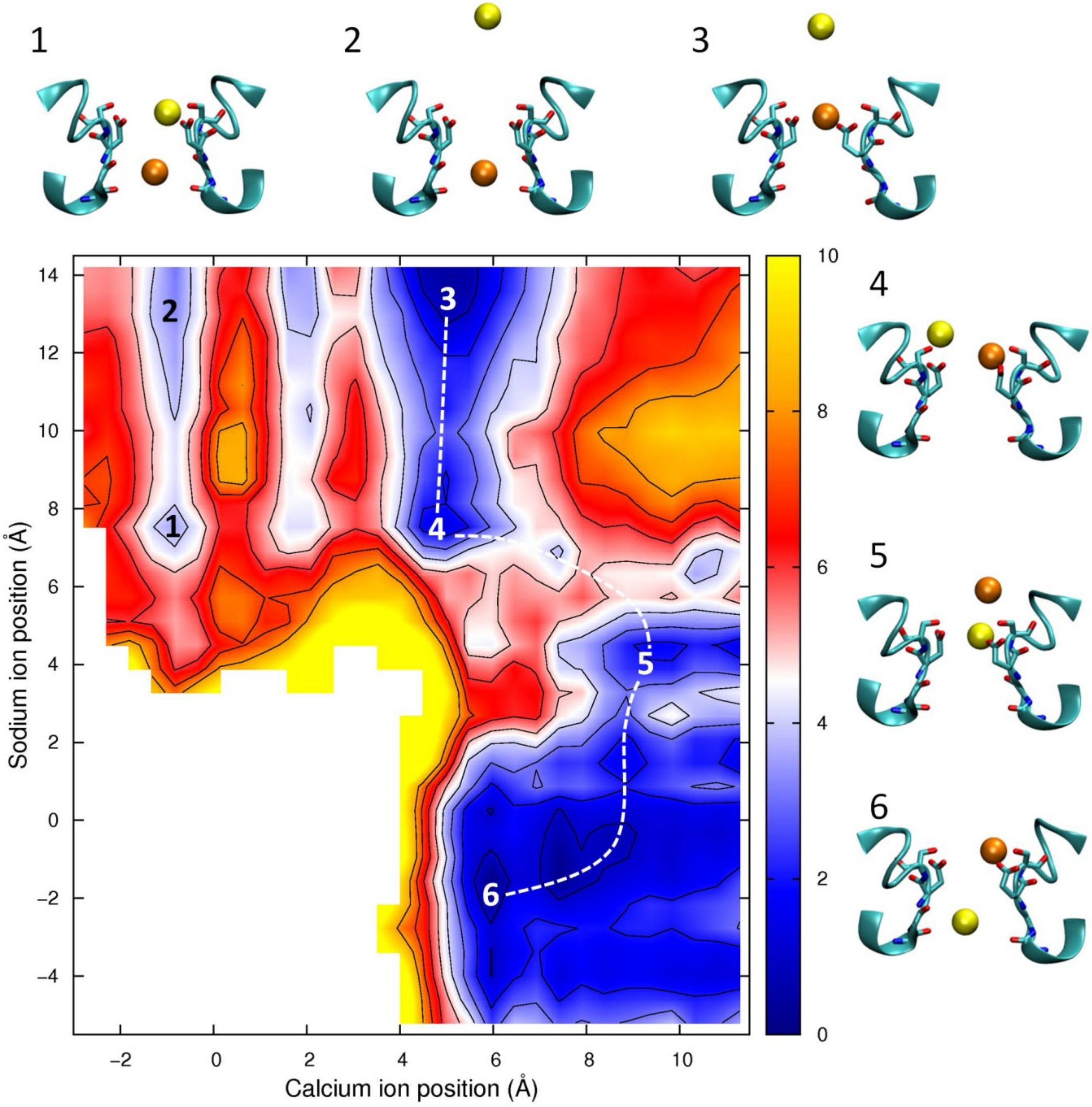

Table 1(on next page)

Energy required to partly dehydrate each ion type

	n								
	0	1	2	3	4	5	6	7	2nd Shell
Na^+	71.2 (1)	47.2 (2)	32.5 (2)	20.9 (3)	11.9 (3)	6.7 (2)	4.0 (3)	N/A	-0.1 (0.2)
Ca^{2+}	312.2 (6)	247.8 (9)	200 (1)	161.6 (6)	123.6 (7)	95 (1)	71.4 (6)	63.6 (7)	11.7 (7)

Table 1: Free energy (kcal/mol) required to partly dehydrate each type of ion. Each value represents the energy to remove an ion from bulk to a situation in which it is surrounded either by *n* water molecules or its first and second solvation shell (column labelled 2nd shell) as determined from FEP simulations. The bracketed values show the standard error in the mean for the last digit calculated from 9 independent simulations.